Journal of Thermal Analysis and Calorimetry (2020) 139:367–374
https://doi.org/10.1007/s10973-019-08377-4

Differential thermal analysis of the antibacterial effect of PLA-based materials planned for 3D printing

P. Maróti[1] · B. Kocsis[2] · A. Ferencz[3] · M. Nyitrai[1,4] · D. Lőrinczy[1]

Received: 9 December 2018 / Accepted: 8 May 2019 / Published online: 21 May 2019

Abstract
Additive manufacturing technologies give many new application possibilities in our everyday life. Biomedical applications benefit a lot from 3D printing. In medical applications, several devices can be easily produced or prototyped with FFF/FDM technologies, but we must minimize the contamination risk. New materials regularly appear on the market, recently specified as antibacterial, resulting from compounded silver nanoparticles. Because scientifically accurate and practical information is not available, this way, we lack information regarding mechanical and thermal stability of the printed products. In addition, these parameters are essential in the setting and optimizing the 3D printers. In our recent study, we aimed to analyze PLA, PLA-HDT as well as PLA-Ag nanocomposite in the form of additive manufacturing filament, with DTA/TG. The results showed that these composites, based on their thermal characteristics, can be suitable for 3D print biomedical devices such as orthoses, casts, medical models and also surgical guides; therefore, their further examination should be important, regarding mechanical characteristics and their possible antibacterial effect.

Keywords Antibacterial · PLA · PLA-HDT and PLA-Ag with silver nanoparticles fibers · 3D medical printing · DTA/TG

Introduction

Recently, manufacturing technique is useful to create physical models for different medical and pharmacological application based on three-dimensional (3D) computed data [1–19]. All these applications strongly rely on material properties such as mechanical and thermal characteristics, biocompatibility, and in the last years, the antibacterial capability became important factor because of the undesirable infections. Parallel with this demand the different sterilization methods used in case of 3D printed models were checked more rigorously [20, 21]. The most frequently used sterilization methods for poly-lactic acid (PLA), which is the favorite among the 3D printing materials, are the follows: (1) steam sterilization (at high pressure and ~ 130 °C), (2) dry sterilization (close to 200 °C), (3) sterilization with radioactive sources and (4) gas sterilization (mainly in ethylene oxide). Their application depends on the local possibilities, but each one has advantage/disadvantage (deformation, degradation, toxic residues, etc.). Of course, the sterilization method and printing temperature are greatly dependent on the thermal characteristics of the most commonly used 3D printing materials. Another important point in the fabrication of PLA-based medical device is the biocompatibility and antibacterial character [22, 23]. The 2009 WHO Guidelines for Safe Surgery summarizes all the evidences and recommendations about perioperative precautions and round of duties [22]. According to it, minimizing contamination in the operating room is essential because generally the environment of interventions can pose a risk to patients.

✉ D. Lőrinczy
denes.lorinczy@aok.pte.hu

[1] Department of Biophysics, Medical School, University of Pécs, Szigeti u. 12, Pécs 7624, Hungary

[2] Department of Medical Microbiology and Immunology, Medical School, University of Pécs, Szigeti u. 12, Pécs 7624, Hungary

[3] Department of Surgical Research and Techniques, Medical Faculty, Semmelweis University, Nagyvárad square 4, Budapest 1089, Hungary

[4] Szentágothai Research Center, University of Pécs, Ifjúság u. 20, Pécs 7624, Hungary

Moreover, medical device development used outside of the operating room must also fulfill the requirements stated in the ISO 10993 series [23]. Overall, minimizing contamination risk is a basic principle in all these cases.

Silver nanoparticles are widely investigated in connection with many different aspects such as antibacterial agents [24–27], its possible antiviral effects [28], its antifungal [29] and antiparasitic activities [30], and all agree on silver ions and silver-based compounds have distinct antimicrobial effects. Adopting these findings to 3D printing is a recent concept that has a limited literature yet, and it is mostly confined on creating custom conductive complex structures [31–33]. A 3D printed antimicrobial medical device study has already been conducted [34], but Sandler et al. used a drug–polymer mixture containing antimicrobial active pharmaceutical ingredient (API) for that purpose. Utilizing silver nanoparticles in 3D printing process as an antimicrobial agent is a novel aspect.

In recent paper, we planned to check the thermal behavior of a novel PLA-Ag, and nanoparticles containing 3D printing materials using TG/DTA in wide temperature range (from 25 to 250 °C), comparing with the data of our previous paper [35]. Simultaneously, we checked their response on the attack of clinically most aggressive bacteria.

Materials and methods

Materials

PLA

We have tested different PLA-based plastic fibers made experimentally with twin-screw extruder by *Filamania LLC/HU* (Limited Liability Company, H-2310 Szigetszentmiklós, Fenyőfa str. 23., Hungary) planned for usage in additive manufacturing technology (FFF/FDM printing). The source of base material was purchased from *NatureWorks LLC/US* (15305 Minnetonka Boulevard Minnetonka, MN 55345 USA). The density of raw material (pellet) was between 1.23 and 1.25 g cm^{-3}, with approx. 67% amorphous and 37% crystalline structure. The D-lactide content—according to NatureWork database—is between 1.2 and 14%; Filamania LLC/HU did not provide the exact value for the tested materials.

PLA-HDT

The base material was the same as in case of PLA; the preheat treatment procedure during the production was made by *Filamania LCC/HU*.

PLA-Ag

It is a PLA-based plastic 3D printing filament mixed with Ag-NPs (NP: nanoparticle). Fabrication was done similarly, as in case of PLA, by the same company. The silver content, the applied colloid and homogeneity of the distribution of the nanoparticles, is a part of the production patent.

In case of printing of all tested materials, the recommended speed of the print head in *X–Y* direction is 60 mm s^{-1} and the thread pull speed is about 15–20 mm s^{-1}. The proposed printing temperature for PLA and its composites is 215 °C, recommended for 100–400-micron print thickness with reduced print head/extruder and tray sink speed.

Bacterial testing

The tested bacteria were: (1) *Micrococcus luteus–Sarcina lutea* ATCC 9341. This bacterium is common in transient skin flora of humans; it can produce carotenoid pigments, resulting in growth of yellow colonies on agar media. The Gram-positive Micrococcal and Bacillus species, e.g., (2) *Bacillus subtilis* ATCC 6633, have industrial uses as bioassay organism for detection of antimicrobial agents. They are occasionally isolated from human clinical specimens where they usually represent contaminants from the skin flora or from the environment [36].

The Gram-positive (3) *Staphylococcus aureus* ATCC 25923, the Gram-negative (4) *Escherichia coli* ATCC 25922 and (5) *Pseudomonas aeruginosa* ATCC 15442, originally were isolated from clinical samples as they are human pathogenic bacteria. They can cause, e.g., wound, respiratory and urinary tract infections [37].

In our experiment, we used BBL™ Mueller–Hinton agar media (Becton, Dickinson and Co. France). The surfaces of media were continuously inoculated with test bacteria; the test disks containing presumably antimicrobial materials were placed on the inoculated surface of the media. After 24 h incubation at 37 °C in a thermostat, the disks were removed and discarded.

TG/DTA measurements

We have used a SSC 5200 SII TG/DTA equipment (made by Seiko, Japan) to study the melting (fusion) properties of the different plastic fibers. The temperature and enthalpy calibration were made by Indium (Alfa Aesar PURATRONIC, Johnson Matthey Company, Ward Hill, MA, USA) using its thermal parameters from Thermal Applications Note TA Instruments (TN-11, Ref. [38]): the heat of fusion was set as 28.57 J g^{-1}, and the melting temperature was taken to be 156.5985 °C [39]. Open aluminum

sample pans of 5 mm diameter were used. The heating rates during the measurements were 10–20–30–40 K min^{-1} from room temperature up to 250 °C, and we applied N_2 gas with 50 mL min^{-1} flow rate. Under the cooling process of melted samples, we did not use external cooler. The average sample mass was 9 ± 1 mg (rounded to integer value).

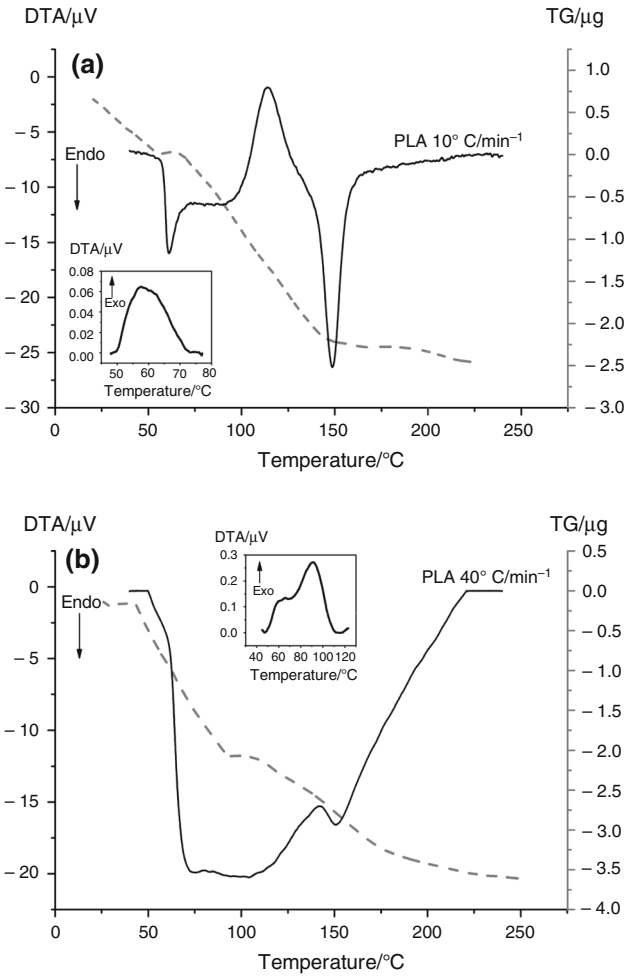

Fig. 1 Heating and (spontaneous) cooling curves (inserts) for PLA base fiber: **a** with 10 °C min^{-1} and **b** with 40 °C min^{-1} heating rate. Solid lines: DTA average curves, dashed lines TG curves. Here and in all further figure too, the endotherm process is downward

Results

The heating test of base PLA, as well as PLA-HDT and PLA-Ag plastic fibers between room temperature and 250 °C, can be seen in Figs. 1–3 (heating rates of 10 and 40 °C min^{-1} are only in all plot, as an average of three trials). The thermal parameters determined from the experimental curves are presented in Tables 1 and 2.

The DTA curves of PLA fiber are demonstrated in Fig. 1a, b. It shows the well-known parts of the polymer heating process: in case of Fig. 1a, a glass transition around 60, crystallization ~ 118, the fusion (melting) at ~ 151 °C. During cooling, a crystallization ~ 61 °C (see Table 1) was observed. Applying 40 °C min^{-1} heating rate, the T_g increased (~ 65 °C), and instead of a definite crystallization peak it could be seen an exo-like range (105–140 °C). During cooling, a double-crystallization peak was produced: a surprising ~ 94 °C, and a shoulder around the heating T_g range. The observed heating/cooling

Table 2 Enthalpy values in heating/cooling cycle of different PLA samples [exo (crystallization) negative and endo (melting or fusion) with positive sign]

	Peak integrals/J g^{-1}		
	Heating		Cooling
	Peak exo.	Peak endo.	Peak exo.
PLA 10 °C min^{-1}	− 17.39	34.41	− 0.32
PLA 40 °C min^{-1}	− 0.11	2.46	− 3.08
PLA-HDT 10 °C min^{-1}	− 20.0	35.2	− 6.2
PLA-HDT 40 °C min^{-1}	− 13.0	20.9	–
PLA-Ag 10 °C min^{-1}	− 27.8	45.5	− 7.57
PLA-Ag 40 °C min^{-1}	− 17.0	26.9	− 6.4

Table 1 Characteristic temperature values in heating/cooling cycle of different PLA fiber samples (T_{on} starting, T_{end} final temperature of process, T_g glass transition temperature, T_{hc} crystallization at heating, T_{cc} crystallization at cooling and T_m melting (fusion) temperatures)

	Heating					Cooling		
	Glass transition			Exo tr.	Endo tr.	Crystallization		
	T_{on}/°C	T_g/°C	T_{end}/°C	T_{hc}/°C	T_m/°C	T_{on}/°C	T_{cc}/°C	T_{end}/°C
PLA 10 °C min^{-1}	56.2	60.1	62.6	117.7	150.5	76.1	61.4	48.9
PLA 40 °C min^{-1}	60.7	64.9	71.5	–	152.4	121.6	94.3	46.6
PLA-HDT 10 °C min^{-1}	56.1	61.5	64.7	97.6	175.7	120.5	98.1	59.8
PLA-HDT 40 °C min^{-1}	63.7	69.1	76.4	120.9	181.4	–	–	–
PLA-Ag 10 °C min^{-1}	55.7	61.8	72.3	96.0	175.0	106.9	91.4	69.6
PLA-Ag 40 °C min^{-1}	63.3	68.4	78.6	118.2	182.5	101.8	88.8	60.7

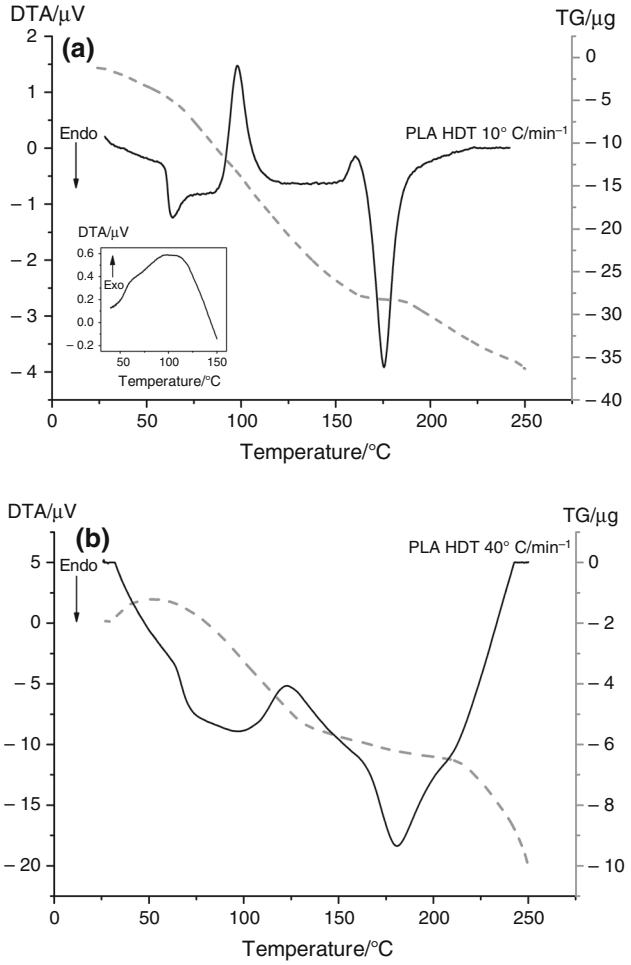

Fig. 2 The melting (fusion) and cooling curves of PLA-HDT (symbols as in Fig. 1). In case of 40 °C min^{-1} heating rate, there was no crystallization in the spontaneous cooling phase

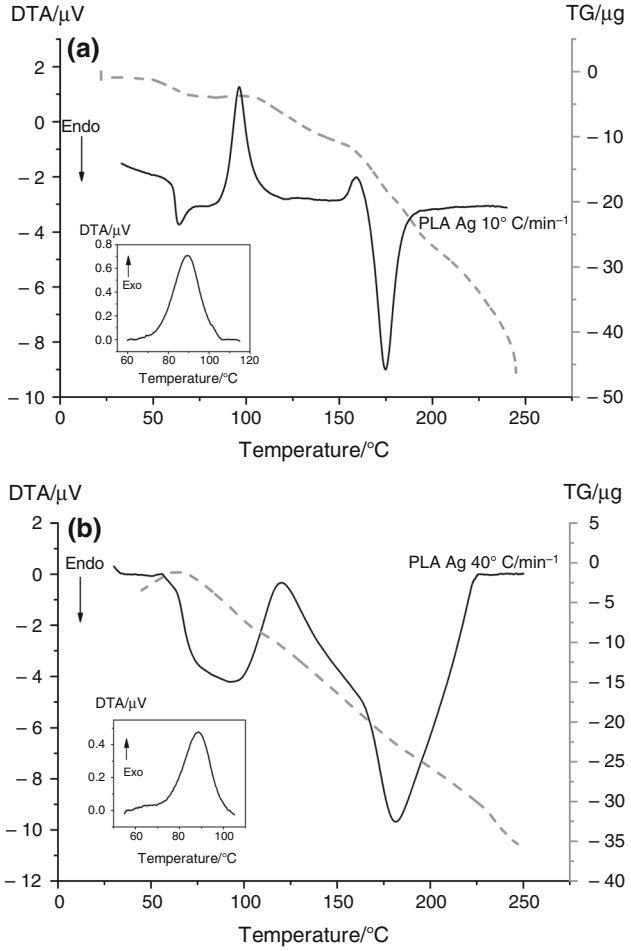

Fig. 3 The TA curves of PLA-Ag nanocomposite fibers (symbols as in Fig. 1)

rate dependence is in a good correlation with data published by Ádám et al. [40].

The transition enthalpies varied strongly in the function of heating rate: both crystallization and melting ones were higher at 10 than at 40 °C min^{-1} rate during heating. It reversed at cooling crystallization. In the investigated temperature range, a remarkable mass loosening cannot waited according to the literature, but a shoulder can be seen at 10 °C min^{-1} rate after the end of glass transition, while at 40 °C min^{-1} rate at the beginning of an "exo-like" jump. After the melting, the mass change was negligible (max. 0.5 µg).

The PLA-HDT fibers (see Fig. 2a, b) showed clearly the effect of preheat treatment. The temperature range of glass transition and the T_g as well as the T_m increased compared to PLA, and all parameters were higher at 40 °C min^{-1} rate. At this heating rate, a definite "baseline" was not achievable after glass transition. The crystallization transition was wider with smaller peak at 40 °C min^{-1} rate. During cooling only at 10 °C min^{-1} rate exhibited crystallization, which also had a shoulder, and its lower compound (see Fig. 2a) was only in the range of T_g. The transition enthalpies were higher in both heating rates than in case PLA. The mass losses were also significantly higher than in PLA.

PLA-Ag nanocomposite (see Fig. 3a, b) showed similar TA characteristics than PLA-HDT during heating. Its thermal parameters were greater than at PLA, exhibiting stronger internal structure caused by Ag nanoparticles. The half width of the transitions was higher, compared with PLA, showing the decreased cooperativity among the structural compounds. The increased enthalpies are reflecting also on the more stable structure. The mass loss was also higher than in PLA in case of both heating rate.

The bacterial test of 3D printed specimens (disks with 15 mm diameter and 5.7 mm height), after their dezincification, provided an unexpected result (see Fig. 4). It was surprising that under the test disks (after its removal) the media were clear, without any colonies. This situation—

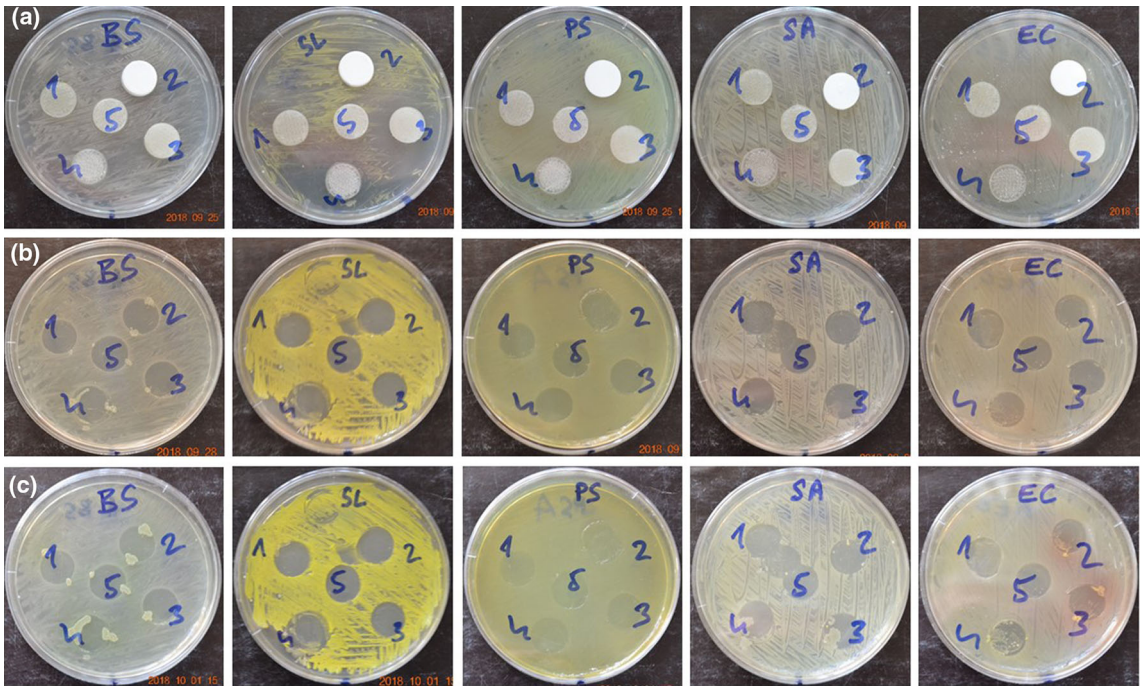

Fig. 4 PLA-based sample disks in different bacterium milieu: Symbols are: bacterial beds BS, *Bacillus subtilis*; SA, *Staphylococcus aureus*; EC, *Escherichia coli*; PS, *Pseudomonas aeruginosa*; SL, *Sarcina lutea*. Printed samples: 1—PLA "Model" (20% $CaCO_3$), 2—PLA, 3—PLA-Ag, 4—PLA "Gypsum" (50% $CaCO_3$), 5—PLA-HDT. Photographs were made 5 days after the removal of disks (row **a**, except of PLA), 8 days of removal (row **b**) and at 11th day (row **c**)

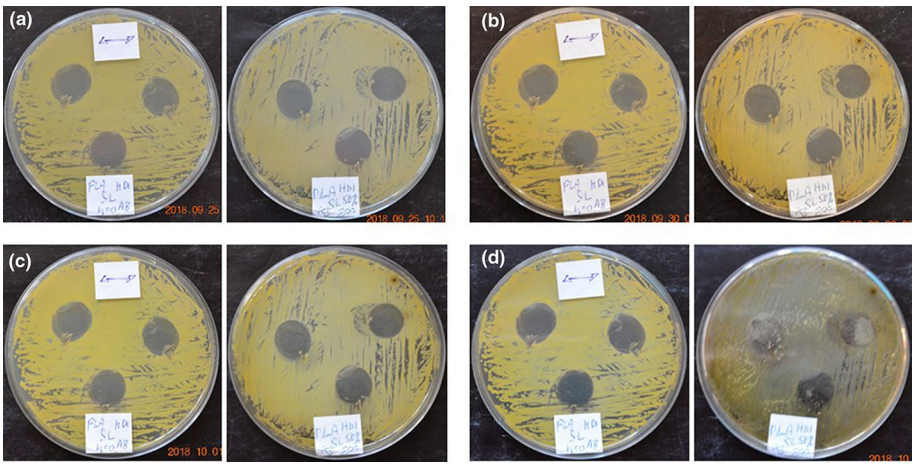

Fig. 5 PLA samples in SL—*Sarcina lutea* bed. Upper left PLA-Ag, upper right PLA-HDT and bottom PLA disks: **a** in 5 days, **b** after 10 days, **c** after 15 days and **d** after 19 days of removing the plastic disks. The two neighbor Petri-disks differ from each other only in the percentage of print completeness

free of colonies—remained for weeks independently from the type of species (see Fig. 5). The best picture (see Fig. 4) developed during *M. luteus* test strain: the yellow colonies and clear zones were impressive. In *P. aeruginosa* test strain, the clear zones were greenish discolored, as this bacterium produces two water-soluble pigments—pyocyanin and fluorescein—and these pigments diffused into the clear zones, and it is difficult to make a good-quality photograph demonstrating that these spots are free of colonies. Sometimes at the site of disk containing test material (No. 4), a few contaminating colonies were found (very probably the reason is the bad removing of the test

sample by forceps, pushing some colony from the base into the original place of the sample).

Discussion

There is an increased interest in medical/pharmacological practice for using the different biodegradable polymers. This way they are frequent objects of different TA analysis. They are appropriate to use (fibers or granules as basic materials) for the microencapsulation of drugs having short biological half-life but frequent administration. It is important the long-term stability of controlled-release dosage forms too [7, 41–44]. The indiscriminate use of antifungal agents has led to the advancement of microorganisms tolerant to the various drugs used in the market [45]. An antibacterial and antioxidant activity of a PLA Nano-silver composite was recently reported [46]. According to our results, the PLA-Ag composite can be used widely in different surgical intervention using 3D printed products, because it has better thermal parameters than PLA (higher T_g, T_{hc}, T_m and T_{cc} as well as calorimetric enthalpy values, see Tables 1, 2). The bacterial test result was very surprising for us because the usual halo ("paraselene") around the printed sample did not appear (see Fig. 4). Instead of it—after removal of sample disks and waiting relative long time—bacteria did not enter into the original place of sample disks from the surrounding (see Figs. 4, 5). Some entrance appeared, but it was the consequence of wrong removal of disks, and under the PLA-$CaCO_3$ composite, a netlike structure appeared, probably as the consequence of looser structure filling.

Conclusions

Technological developments made a revolution and play a central role in the improvements of medical methods. The most commonly used PLA is well-characterized material in science, but the thermal and mechanical properties of the composites based on its application have been not well described yet. Our present results have showed that the investigated PLA-HDT and PLA-Ag can be potentially used in most biomedical applications. These results also highlighted to the careful but essential sterilization processes during development and application of surgical implants and tools. Because of the unmissable sterilization process, the thermal structural stability of the material remains a key point. It means that disinfection at high temperature should be avoided. Thus, HDT-PLA and PLA-Ag can be promising materials as a base material for composites suitable for heat-based sterilization methods. The strange antibacterial effect of the tested samples is also interesting; this way the infections after implantation of printed elements could be minimalized. The experimental setting used in our present study has several advantages to assess the quality and safety of 3D printed materials, and thus, it deserves further attention in order to determine the detailed protocol and processes necessary for possible future therapeutic use.

Acknowledgements Open access funding provided by University of Pécs (PTE). The authors express their thanks to Jürgen Koch (THASS, Thermal Analysis & Surface Solutions GmbH, Freiburg—Germany) for his help in obtaining the instrument, and to Dr. Zsolt Bodnár for providing the test materials. Special thanks to Medical School, University of Pécs Research Fund Grant (A. Ferencz, PTE ÁOK KA 114/603/2009). Thanks for P. Varga, to help in the producing and dezincification of the printed samples as well as thanks for Z. Ujfalusi to help in the drawing of TA/TG figures. This research was supported by a grant from the National Research, Development and Innovation Office and the European Union (GINOP 2.3.2-15-2016-00022).

References

1. Rengier F, Mehndiratta A, von Tengg-Kobligk H, Zechmann CM, Unterhinninghofen R, Kauczor HU, Giesel FL. 3D printing based on imaging data: review of medical applications. Int J CARS. 2010;5:335–41.
2. Ventola CL. Medical applications for 3D printing: current and projected uses. Pharm Therap. 2014;39(10):704–11.
3. Norman J, Madurawe RD, Moore CMV, Khan MA, Khairuzzaman A. A new chapter in pharmaceutical manufacturing: 3D-printed drug products. Adv Drug Deliv Rev. 2017;108:39–50. https://doi.org/10.1016/j.addr.2016.03.001.
4. Trombetta R, Inzana JA, Schwarz EM, Kates SL, Awad HA. 3D printing of calcium phosphate ceramics for bone tissue engineering and drug delivery. Ann Biomed Eng. 2017;45(1):23–44. https://doi.org/10.1007/s10439-016-1678-3.
5. Skowyra J, Pietrzak K, Alhnan MA. Fabrication of extended-release patient-tailored prednisolone tablets via fused deposition modelling (FDM) 3D printing. Eur J Pharm Sci. 2015;68:11–7. https://doi.org/10.1016/j.ejps.2014.11.009.
6. Gottnek M, Pintye-Hódi K, Regdon G Jr. Tracking of the behaviour of lidocaine base containing hydroxypropylcellulose free films with thermoanalytical method. J. Therm Anal Calorim. 2015;120:201–8.
7. Regdon G Jr, Korteby Y. Quantitative and qualitative use of thermal analysis for the investigation of the properties of granules during fluid bed melt granulation. J Therm Anal Calorim. 2018;133:619–32. https://doi.org/10.1007/s10973-017-6848-5.
8. Ferencz A, Fehér D, Szabó G, Dankó T, Juhos K, Szentes P, Csukás D, Sándor J, Ender F, Fónagy L, Molnár K, Jedlovszky-Hajdú A, Zrínyi M, Wéber G. Abdominal hernia repair with poly (succinimide) and with its cysteamine crosslinked nanofiber

hernia meshes. A preliminary experimental study. Int J Biol Technol Res. 2016;2:1–6.
9. Hermsen JL, Burke TM, Seslar SP, Owens DS, Ripley BA, Mokadam NA, et al. Scan, plan, print, practice, perform: development and use of a patient-specific 3-dimensional printed model in adult cardiac surgery. J Thorac Cardiovasc Surg. 2016;153(1):132–40. https://doi.org/10.1016/j.jtcvs.2016.08.007.
10. Mobbs RJ, Coughlan M, Thompson R, Sutterlin CE, Phan K. The utility of 3D printing for surgical planning and patient-specific implant design for complex spinal pathologies: case report. J Neurosurg Spine. 2017;26(4):513–8. https://doi.org/10.3171/2016.9.spine16371.
11. Nyberg EL, Farris AL, Hung BP, Dias M, Garcia JR, Dorafshar AH, et al. 3D-printing technologies for craniofacial rehabilitation, reconstruction, and regeneration. Ann Biomed Eng. 2017;45(1):45–57. https://doi.org/10.1007/s10439-016-1668-5.
12. Tetsworth K, Block S, Glatt V. Putting 3D modelling and 3D printing into practice: virtual surgery and preoperative planning to reconstruct complex post-traumatic skeletal deformities and defects. SICOT-J. 2017;3:16. https://doi.org/10.1051/sicotj/2016043.
13. Angus P Fitzpatrick* MIM, Collins PK, Gibson I. Design of a patient specific, 3D printed arm cast. In: The international conference on design and technology: DesTech Conference Proceedings; 2017. p. 135–42.
14. David P, Jiri R, Daniel K, Pavel S, Tomas N. Pilot study of the wrist orthosis design process. Rapid Prototyp J. 2014;20(1):27–32. https://doi.org/10.1108/rpj-03-2012-0027.
15. Lin H, Shi L, Wang D. A rapid and intelligent designing technique for patient-specific and 3D-printed orthopedic cast. 3D Print Med. 2016;2(1):4. https://doi.org/10.1186/s41205-016-0007-7.
16. Mavroidis C, Ranky RG, Sivak ML, Patritti BL, DiPisa J, Caddle A, et al. Patient specific ankle-foot orthoses using rapid prototyping. J NeuroEng Rehabil. 2011;8(1):1. https://doi.org/10.1186/1743-0003-8-1.
17. Szebényi G, Czigány T, Magyar B, Karger-Kocsis J. 3D printing-assisted interphase engineering of polymer composites: concept and feasibility. Express Polym Lett. 2017;11(7):525–30. https://doi.org/10.3144/expresspolymlett.2017.50.
18. Malik HH, Darwood ARJ, Shaunak S, Kulatilake P, El-Hilly AA, Mulki O, et al. Three-dimensional printing in surgery: a review of current surgical applications. J Surg Res. 2015;199(2):512–22. https://doi.org/10.1016/j.jss.2015.06.051.
19. Leonardo C, Massimiliano F, Francesca DC, Franco P, Roberto S. Computer aided design and manufacturing construction of a surgical template for craniofacial implant positioning to support a definitive nasal prosthesis. Clin Oral Implant Res. 2011;22(8):850–6. https://doi.org/10.1111/j.1600-0501.2010.02066.x.
20. Block SS, editor. Disinfection, sterilization, and preservation. Philadelphia: Lippincott Williams & Wilkins; 2001. p. 79–135.
21. Athanasiou KA, Niederauer GG, Agrawal CM. Sterilization, toxicity, biocompatibility and clinical applications of polylactic acid/polyglycolic acid copolymers. Biomaterials. 1996;17(2):93–102.
22. WHO Guidelines for Safe Surgery 2009: safe surgery saves lives. World Health Organization, Geneva; 2009. http://apps.who.int/iris/.
23. ISO 10993 series. https://www.iso.org/ics/11.100.20/x/.
24. Ivan S, Branka SS. Silver nanoparticles as antimicrobial agent: a case study on *E. coli* as a model for Gram-negative bacteria. J Colloid Interface Sci. 2004;275(1):177–82.
25. Kim JS, Kuk E, Yu KN, Kim JH, Park SJ, Lee HJ, Kim SH, Park YK, Park YH, Hwang CY, Kim YK, Lee YS, Jeong DH, Cho MH. Antimicrobial effects of silver nanoparticles. Nanomed Nanotechnol Biol Med. 2007;3(1):95–101.
26. Mahendra R, Alka Y, Aniket G. Silver nanoparticles as a new generation of antimicrobials. Biotechnol Adv. 2009;27(1):76–83.
27. Morones JR, Elechiguerra J, Camacho A, Holt K, Kouri JB, Ramírez JT, Yacaman MJ. The bactericidal effect of silver nanoparticles. Nanotechnology. 2005;16(10):2346–53.
28. Jose LE, Justin LB, Jose RM. Interaction of silver nanoparticles with HIV-1. J Nanobiotechnol. 2005;3(6):1–10.
29. Panácek A, Kolár M, Vecerová R, Prucek R, Soukupová J, Krystof V, Hamal P, Zboril R, Kvítek L. Antifungal activity of silver nanoparticles against *Candida spp*. Biomaterials. 2009;30(1):6333–40.
30. Marimuthu S, Rahuman AA, Rajakumar G, Santhoshkumar T, Kirthi AV, Jayaseelan C, Bagavan A, Zahir AA, Elango G, Kamaraj C. Evaluation of green synthesized silver nanoparticles against parasites. Parasitol Res. 2011;108:1541–9.
31. Hsien HL, Kan SC, Kuo CH. Inkjet printing of nanosized silver colloids. Nanotechnology. 2005;16(10):2436–41.
32. Fantino E, Chiappone A, Roppolo I, Manfredi D, Bongiovanni R, Pirri CF, Calignano F. 3D printing of conductive complex structures with in situ generation of silver nanoparticles. Adv Mater. 2006;28:3712–7.
33. Mannoor MS, Jiang Z, James T, Kong YL, Malatesta KA, Soboyejo WO, Verma N, Gracias DH, McAlpine MC. 3D printed bionic ears. Nano Lett. 2013;13(6):2634–9.
34. Sandler N, Salmela I, Fallarero A, Rosling A, Khajeheian M, Kolakovic R, Genina N, Nyman J, Vuorela P. Towards fabrication of 3D printed medical devices to prevent biofilm formation. Int J Pharm. 2014;459:62–4.
35. Maróti P, Varga P, Ferencz A, Ujfalusi Z, Nyitrai M, Lőrinczy D. Testing of innovative materials for medical additive manufacturing by DTA. J Therm Anal Calorim. 2018. https://doi.org/10.1007/s10973-018-7839-x.
36. Winn W Jr, Allen S, Janda W, Koneman E, Procop G, Schreckenberger P, Woods G, editors. Koneman's color atlas and textbook of diagnostic microbiology. 6th ed. Philadephia: Lippincott Williams & Wilkins; 2006.
37. Mandell D. Bennett's principles and practice of infectious diseases. 8th ed. New York: Elsevier; 2015 (**Editors: John E. Bennett, Raphael Dolin, Martin J. Blaser**).
38. Preston-Thomas H. The international temperature scale of 1990 (ITS-90). Metrologia. 1990;27(2):107.
39. Neches RY, Flynn KJ, Zaman L, Tung E, Pudlo N. On the intrinsic sterility of 3D printing. Peer J. Preprints. 2016;4:e542v2. https://doi.org/10.7287/peerj.preprints.542v2.
40. Ádám B, Ádámné -Major A. Non-isotherm testing of PLA filament of 3D printing by DSC. Gradus. 2016;3:166–72 (**in Hungarian**).
41. Hekmatara T, Regdon G Jr, Sipos P, Erős I, Pintye-Hódi K. Thermoanalytical study of microspheres containing diltiazem hydrochloride. J Therm Anal Calorim. 2006;86(2):287–90.
42. Regdon G Jr, Kósa A, Erős I, Pintye-Hódi K. Thermoanalytical behaviour of some coating free films. J Therm Anal Calorim. 2007;89(3):793–7.
43. Regdon G Jr, Hegyesi D, Pintye-Hódi K. Thermal study of ethyl cellulose coating films used for modified release (MR) dosage forms. J Therm Anal Calorim. 2012;108:347–52.
44. Gottnek M, Pintye-Hódi K, Regdon G Jr. Tracking of the behaviour of lidocaine base containing hydroxypropylcellulose free

films with thermoanalytical method. J Therm Anal Calorim. 2015;120:201–8.
45. de Lima Ramos FJ, Jr Alves da Silva KM, Brandao DO, et al. Investigation of the thermal behavior of inclusion complexes with antifungal activity. J Therm Anal Calorim. 2018;133:641–8.
46. Munteanu BS, Aytac Z, Pricope GM, Uyar T, Vasile C. Polylactic acid (PLA)/silver-NP/Vitamin E bionanocomposite electrospun nanofibers with antibacterial and antioxidant activity. J Nanopart Res. 2014;16(2643):1–12.